PCCP

Accepted Manuscript

ROYAL SOCIETY OF CHEMISTRY

www.rsc.org/pccp

Journal Name

ARTICLE

Mechanistic investigation of the trimethylamine-N-oxide reduction catalysed by biomimetic molybdenum enzyme models

Received 00th January 20xx,
Accepted 00th January 20xx

DOI: 10.1039/x0xx00000x

www.rsc.org/

M. Fortino,[a] T. Marino,*[a] N. Russo,[a] E. Sicilia*[a]

In this paper, we report a theoretical investigation of the reduction reaction mechanism of Me_3NO by molybdenum containing systems that are functional and structural analogues of trimethylamine N-oxide reductase mononuclear molybdenum enzyme. The reactivity of monooxomolybdenum(IV) benzenedithiolato complex and its derivatives with carbamoyl (t-BuNHCO) and acylamino (t-BuCONH) substituents on the benzene rings in both *cis* and *trans* arrangements was explored. Calculated energy profiles describing the steps of two mechanisms of attack considered viable (named *cis*- and *trans*-attack) by the Me_3NO substrate at *cis* and *trans* positions with respect to the oxo ligand show that the attack in *cis* is energetically more favourable tha the attack in *trans*. Along the pathway for the *cis*-attack the first step of the reaction, that is rate-determining for all the studied compounds, is the approach of the substrate to the Mo centre in *cis* to the oxo ligand that causes a distortion of the initial square-pyramidal geometry of the complex. The reaction steps involved in the *trans* position attack were also explored. Calculations confirm that, as previously suggested, the introduction of ligands able to form intramolecular NH···S hydrogen bonds accelerates the reduction of the Me_3NO substrate and contributes to the tuning of the reactivity of molybdoenzyme models.

1. Introduction

Enzymes are essential for the life since they possess phenomenal capability to catalyse efficiently a huge number of reactions with high specificity and are able to work under mild and physiological conditions. Understanding how enzymes achieve these remarkable results is of fundamental significance in biochemistry. In fact, it can also contribute to develop more efficient inhibitors, to predict the drugs metabolism and to design new catalysts for specific reactions.[1-5]

The high efficiency of natural enzymes inspired the development of so called biomimetic catalysts that mimic the active sites of natural enzymes in order to promote catalysis in homogeneous phase.[6] Furthermore, discovering how the natural enzymes work allows to design artificial enzymes with superior catalytic power.[6-10]

In metal-containing enzymes the active site is characterized by the presence of a metal cation coordinated to specific amino acid residues and represents the core of the catalytic event.[11] This "catalytic core" is the reference for designing new biomimetic organometallic complexes with high catalytic efficiency. Nakamura an co-workers[12] and Okamura et al.[13-15] showed as a series of bio-inspired monooxomolybdenum(IV) complexes are able to catalyse the reduction of trimethylamine-N-oxide (Me_3NO) to trimethylamine (Me_3N) mimicking the activity of the trimethylamine-N-oxide reductase (TMAOR) enzyme. This enzyme belongs to the molybdenum containing family whose catalytic centre contains one or two pyranopterin dithiolene ligands, called molybdopterin cofactors, coordinated by the dithiolene sulphur atoms to the metal ion (Scheme 1). TMAOR is implicated in the catalysis of oxygen atom transfer reactions according to the following equation:[16-18]

$$Mo^{IV}OL_n + XO \rightarrow Mo^{VI}O_2L_n + X \quad (1)$$

The originally synthesized biomimetic TMAOR enzymes were characterized by the presence of the 1,2-benzenedithiolato (bdt) ligands in state of the natural pyranopterin dithiolene moieties (see Scheme 1a).[13]

Successively, Okamura's group investigated the role played by NH···S hydrogen bonds for sulphur atoms bonded to the molybdenum[13] and demonstrated that the introduction of four intramolecular NH···S hydrogen bonds into a monooxomolybdenum(IV) complex $(NEt_4)_2[Mo(IV)O(bdt)_2]$ accelerates the reduction of Me_3NO to Me_3N along with the production of the corresponding dioxomolybdenum(VI) complex. More recently, in Okamura's laboratory[14,15] new series of monooxomolybdenum(IV) complexes containing only two NH···S hydrogen bonds were synthetized. In the first series, a carbamoyl group (RNHCO) was used (Scheme 1b) to introduce an amide moiety that led to the formation of a flexible NH···S hydrogen bond

[a] *Department of Chemistry and Chemical Technologies, Università della Calabria, 87036, Arcavacata di Rende, Italy.*
† M. Fortino, Prof. Dr. T. Marino, Prof. N. Russo, Prof. Dr. E. Sicilia
*tmarino@unical.it ; siciliae@unical.it .
Electronic Supplementary Information (ESI) available: [details of any supplementary information available should be included here]. See DOI: 10.1039/x0xx00000x

and resulted in a small contribution to the reduction of Me_3NO in polar solvent.[14]

For the next series, instead, new ligands with acylamino groups (RCONH), as shown in Scheme 1c, were designed and synthesized.[15] In this case, the formed five-membered hydrogen bond, reminiscent of the intraligand interaction in the molybdopterin cofactor, allowed a better investigation of the relationship between the strength of the hydrogen bond and the reactivity of the molybdoenzyme models.

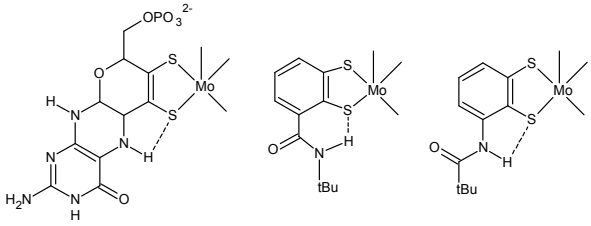

Scheme 1. Molybdopterin ligand a) present in the natural enzyme, compared with carbamoyl b) and acylamino c) groups containing model ligands.

For the Me_3NO reduction by such monooxomolybdenum(IV) complexes two reaction mechanisms are viable.[13,14] In the traditional mechanism,[13] the attack by Me_3NO to Mo takes place at the position *trans* to the oxo ligand to yields an intermediate Me_3NO adduct. After that, the trimethylamine N-oxide ligand moves to the *cis* position through a *trans-cis* rearrangement and by the N-O bond dissociation a *cis*-dioxomolybdenum(VI) complex is formed. The *trans-cis* rearrangement becomes the rate-determining step at high Me_3NO concentrations when the substituent is bulky or the intermediate is stabilized. The alternative mechanism[14] involves direct Me_3NO cis attack to Mo when very bulky groups hamper the trans-cis rearrangement. For the sake of clarity, from now on, the former mechanism will be indicated as *trans*-attack and the latter as *cis*-attack.

We present here the outcomes of a detailed theoretical Density functional investigation of the proposed reaction mechanisms for the oxo transfer from Me_3NO to the monooxomolybdenum(IV) benzenedithiolato complex, $[Mo(IV)O\text{-}(bdt)_2]^{2-}$ labelled E, and its $[Mo(IV)O\text{-}(1,2\text{-}S2\text{-}3\text{-}t\text{-}BuNHCOC_6H_3)_2]^{2-}$, $E_{(carb)}$ and $[Mo(IV)O\text{-}(1,2\text{-}S2\text{-}3\text{-}t\text{-}BuCONHC_6H_3)_2]^{2-}$, $E_{(acylam)}$, derivatives. A comparative analysis was performed with the aim to elucidate the influence on the course of the reaction of both the presence of substituents on the benzene ring and formation of NH···S hydrogen bonds. Such kind of studies is useful to shed light on the behavior of the real enzymes, in spite of the sophisticated structure of the active site, which would require the inclusion of additional species and interactions in the surrounding media. In the present case the comparison between the behavior of the complex with unsubstituted 1,2-benzenedithiolato ligands with those of complexes having substituents able to form NH···S hydrogen bond allows to deduce useful information on the role such hydrogen bond interactions play in influencing the reactivity of real enzymes.

Trans- and *cis*-mechanisms were explored for all the complexes, whereas for $\mathbf{E_{(carb)}}$ and $\mathbf{E_{(acylam)}}$ monooxomolybdenum(IV) complexes the reactivity of both *cis* and *trans* isomers was examined.

Moreover, the structure and stability of the formed dioxomolybdenum(VI) complexes were carefully checked for confirming whether products exist as a single isomer, where both oxo ligands are *trans* to each of the two hydrogen-bonded thiolate ligands.

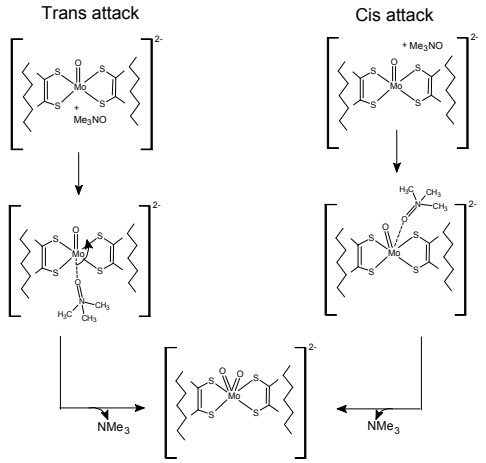

Scheme 2. Schematic representation of the reaction steps for the *trans*- and *cis*-attack mechanisms.

All calculations were carried out with the support of the information coming from experiments and previous theoretical investigations of the reactivity of molybdenum enzymes.[19-23] A summary of all the alternatives examined here is shown in Scheme 3.

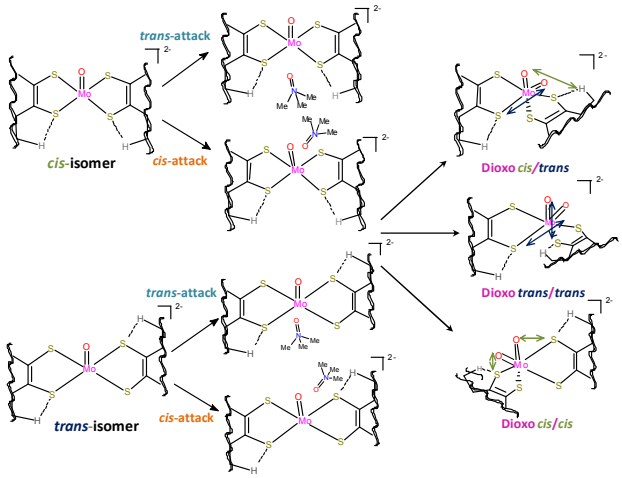

Scheme 3. Schematic representation of the mechanistic alternatives for the Me_3NO attack to *cis* and *trans* isomers of monooxomolybdenum(IV) complexes .

2. Computational methods

Molecular geometry optimizations were carried out without symmetry constraints at the density functional level of theory, by using the Gaussian 09 code[24] employing the M06-L[25] functional, that is recommended for the calculation of transition metal containing systems thermochemistry.[26] Additional B3LYP[27,28] and OPBE[29]

preliminary calculations were performed to check the singlet ground state multiplicity of the examined complexes. The standard 6-31+G(d,p) basis set was used for the C, N, O, S, and H atoms, whereas the SDD pseudo-potential, properly designed to replace core electrons, reduce the computational effort and advantageously include relativistic and other effects, in connection with the relative orbital basis set[30] was employed for the molybdenum atom. Although also higher quality basis sets were used, we concluded that the chosen 6-31+G(d,p) basis sets represent a proper compromise, due to the size and the number of the investigated complexes, between the computational cost and the accuracy of the results. For transition states, in particular, is crucial the choice of suitable basis sets that allow to carry out a great number of calculations for their location. In addition, we have checked the influence of the use of a full-electron basis set for the metal centre on both the geometrical structures and energetics and verified that changes are not significant. All of the reported structures represent genuine minima or transition states on the respective potential energy surfaces, as confirmed by analysis of the corresponding Hessian matrices. For transition states, the vibrational mode associated with the imaginary frequency was verified to be related to the correct movement of involved atoms. Furthermore, the IRC[31,32] method was used to asses that the localized TSs correctly connect to the corresponding minima along the imaginary mode of vibration. The influence of dimethylformamide (DMF) solvent effects on the energetics of the process was estimated in the framework of the SMD[33] model. Single-point calculations on all stationary points structures obtained from gas-phase calculations by using the same M06-L and basis sets computational approach were performed. Calculated reaction Gibbs free energies in solution, ΔG_{sol}, for each process were obtained as the sum of two contributions: a gas-phase reaction free energy, ΔG_{gas}, and a solvation reaction free energy term calculated with the SMD approach, ΔG_{solv}. NBO[34,35] analysis of the charge density was performed for some key species intercepted along the reaction paths.

3. Results

3.1. Me_3NO reduction by the $[Mo(IV)O(bdt)_2]^{2-}$ complex

The potential energy surface (PES) calculated to describe the oxo transfer from the Me_3NO substrate to the Mo(IV) bis-dithiolene $[Mo(IV)O(bdt)_2]^{2-}$ complex is depicted in Figure 1 together with the stationary points optimized structures. The values of the most relevant geometrical parameters of minima and transition states can be found in Figure S1 of the Electronic Supporting Information (ESI) together with atomic Cartesian coordinates (Table S1). Preliminary computations were performed considering different spin multiplicities for the reaction of Me_3NO with the monooxomolybdenum(IV) benzenedithiolato-Mo complex. Results show that the singlet is the ground state and the triplet the first excited state along the entire PES and no crossing between the two electronic spin states occurs (see Figure S2, in the ESI). In particular, the calculated energy difference between the ground singlet and the excited triplet states is 15.2 kcal mol^{-1} for the **ES** complex.

Experimental investigations suggest that a second order kinetics is followed[36] and many examples are reported of *cis*-attack.[19,21-23] In spite of such evidence both *cis*- and *trans*-attack mechanisms were explored even if all the attempts to locate the stationary points along a pathway describing a *trans*-attack failed. This result agrees with molybdenum chemistry[37,38] that does not allow the formation, albeit transient, of a linear dioxo species as a consequence of a *trans* attack. The main cause of this behavior lies in the strengths of the M=O bonds that, for a d^0 configuration, require a bent structure to maximize orbital interactions. As a consequence, only the PES for the singlet ground state describing the *cis*-attack is reported.

Me_3NO approaches the **E** complex causing a distortion of the initial square pyramidal geometry of the complex. A transition state lying 18.1 kcal mol^{-1} in DMF solvent above the reference energy of separated reactants (**E**+**S**) was intercepted corresponding to the movement of one of the sulfur atoms from its position to allow the oxygen atom of Me_3NO to enter the coordination sphere of the Mo centre. The distance between the substrate oxygen and the Mo(IV) centre is 2.345 Å. The **ES** first adduct, stabilized by only 1.8 kcal mol^{-1} with respect to the transition state leading to it, is formed.

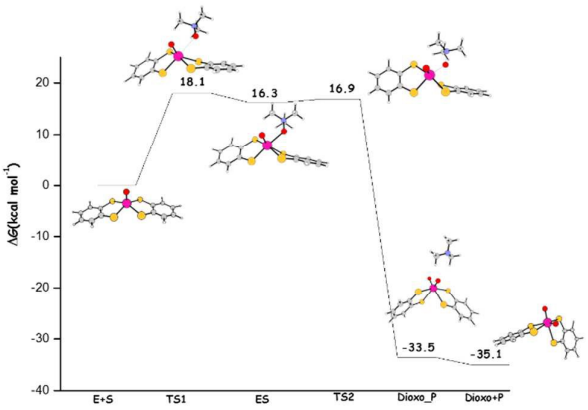

Figure 1. Calculated M06-L *cis*-attack free energy profile for the monooxomolybdenum(IV) benzenedithiolato complex (**E**). Energies are in kcal mol^{-1} and relative to reactants' asymptote.

As a consequence of the distortion of the initial geometry, the bond distance between Mo and the S atom in *trans* position with respect to the M=O bond increases from 2.440 Å to 2.740 Å (Figure S1) and the O-Mo-S valence angle changes from 108.3° to 156.0°. The reaction proceeds toward the product formation by overcoming a very low energy barrier, only 0.6 kcal mol^{-1} for a transition state that corresponds to the formation of a new Mo-O (2.058 Å) bond and the definitive cleavage of the N-O (1.547 Å) substrate bond.

The vibrational N-O stretching mode associated to the imaginary frequency (570*i* cm^{-1}) well accounts for this event. From the computed PES it is clear that the most energy demanding step is the formation of the **ES** complex, whereas once the **ES** adduct is formed the reduction of Me_3NO and the oxidation of Mo easily occurs.

Me_3NO reduction by the $[Mo(IV)O\text{-}(1,2\text{-}S2\text{-}3\text{-}t\text{-}BuNHCOC_6H_3)_2]^{2-}$, $E_{(carb)}$, complex

In their detailed experimental investigations Okamura and collaborators demonstrated as the introduction of intramolecular NH···S hydrogen bonds[14] can stabilize the intermediate in the reduction path of Me_3NO resulting in more favourable reaction kinetics. In this section what is the effect of the unsymmetrical introduction of t-BuNHCO groups on both benzene rings of 1,2-benzenedithiolato ligands is examined and the reactivity of both *cis* and *trans* isomers is investigated. M06-L fully optimized structure of the *trans*-$\mathbf{E}_{(carb)}$ complex is shown in Figure 2, where the experimental and theoretical values of the most significant geometrical parameters are compared. Calculated geometrical parameters agree with those extracted from the crystallographic characterization[14] of the complex indicating a good modeling of the investigated systems. The main deviation concerns, as expected, the NH···S hydrogen bond distances that seem to be underestimated at theoretical level. This apparent discrepancy can be explained considering that calculations allow a more secure location of the hydrogen atoms involved in the NH···S hydrogen bonding interaction with respect to the values extracted from the crystallographic characterization of the complex where a fixed N-H distance of 0.881 Å is assumed. In fact, if we compare the N···S distances, the agreement between theory and experiment (see Figure 2) becomes quite good. Supporting Information gives atomic coordinates for the complex (Table S2). More detailed geometrical information for all the intercepted stationary points are reported in Figure S3 of the SI.

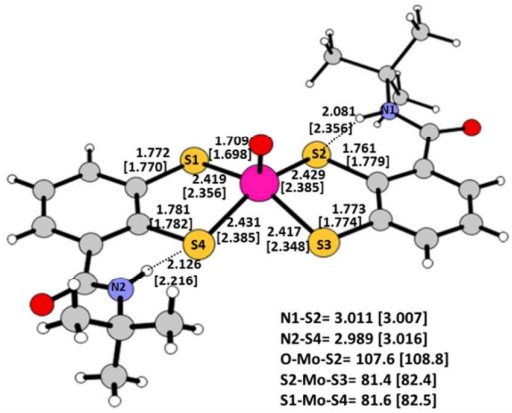

Figure 2. M06-L optimized structure of $\mathbf{E}_{(carb)}$ in its *trans* arrangement. Selected bond lengths (in Å) and angles (degrees) are compared with available experimental values in square brackets.

In contrast to what occurred in the unsubstituted **E** complex, intramolecular NH···S hydrogen bond formation makes the Mo-S bonds distinguishable as (see Figure 2) the Mo-S bond with S2 and S4 sulphur atoms involved in the hydrogen bonds are longer than the Mo-S bond distances with S1 and S3 atoms. Reaction pathways for both *cis*, *cis*-$\mathbf{E}_{(carb)}$ and *trans*, *trans*-$\mathbf{E}_{(carb)}$ isomers were investigated together with the identity of the products, according to ^{1}H NMR analysis and DFT calculations,[14] that proposed a single isomer to be formed in which both oxo ligands are *trans* to each of the two hydrogen-bonded thiolate ligands. Moreover, for each isomer both *cis*- and *trans*-attack mechanisms were explored. The calculated *cis*-attack free energy profiles for the Me_3NO reduction assisted by *cis*-$\mathbf{E}_{(carb)}$, and *trans*-$\mathbf{E}_{(carb)}$ isomers are depicted in **Path a** and **Path b,** respectively of Figure 3. The PES describing the *trans*-attack reaction steps for the *cis*-$\mathbf{E}_{(carb)}$ complex is shown in Figure 4, whereas the PES for the *trans*-attack on the *trans*-$\mathbf{E}_{(carb)}$ complex can be found in the ESI (Figure S4) together with detailed geometrical information (Table S3 and Figure S5). The two *cis* and *trans* isomers result to be isoenergetic in agreement with a previous gas-phase theoretical investigation on these two conformers employing the B3LYP exchange-correlation functional.[14] The reaction evolves following the same steps described for the **E** unsubstituted Mo(IV) complex for both *cis* and *trans* isomers. It is worth underlining that for the ***cis*-$\mathbf{E}_{(carb)}$** complex the attack takes place from the unhindered side of the complex with sulphur atoms not involved in hydrogen bonds. Due to the symmetric disposition of the t-BuNHCO groups with respect to the Mo centre in the *trans*-$\mathbf{E}_{(carb)}$ complex, instead, for the coordination of the substrate the side of attack is unimportant, whereas different results are obtained whether the hydrogen-bonded sulphur is involved (i.e. S2 or S4 in Figure 2) or not (i.e. S1 or S3 in Figure 2).

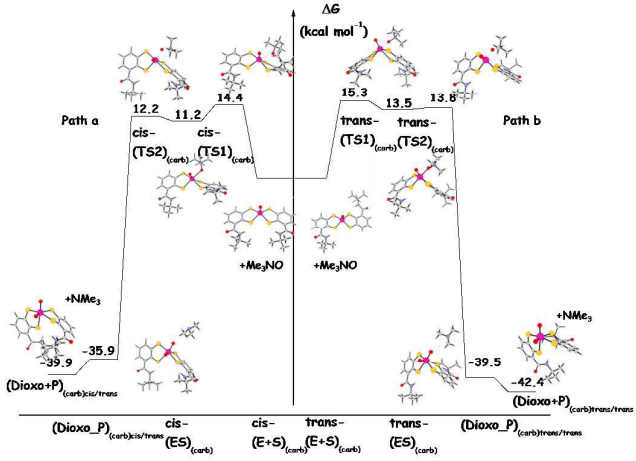

Figure 3. Calculated M06-L free energy profiles for the **Me_3NO** *cis*-attack to the monooxomolybdenum(IV) $\mathbf{E}_{(carb)}$ complex in its *cis* (**Path a**) and *trans* (**Path b**) arrangements. Energies are in kcal mol^{-1} and relative to reactants' asymptote.

From the exploration of both possibilities resulted that the attack from the side of the hydrogen-bonded sulphur is the preferred one and, hence, in the next paragraphs the corresponding lowest energy pathway will be described. The *cis*-attack of the Me_3NO substrate to the metallic centre causes a distortion of the initial square pyramidal geometry and, as a consequence, to form the first weakly bound adducts between the *cis*-$\mathbf{E}_{(carb)}$ and *trans*-$\mathbf{E}_{(carb)}$ complexes and Me_3NO the overcoming of a transition state barrier is required. The height of the barrier is 14.4 kcal mol^{-1} along the **Path a** for the *cis* isomer and 15.3 kcal mol^{-1} along the **Path b** for the *trans* isomer. The formed intermediates are more stable by only a few kcal mol^{-1} than the preceding transition states and even smaller is the difference in energy with respect to the next transition states. By surmounting the second transition state barrier the N-O bond is definitively broken and a new Mo-O bond is formed. The analysis of the

imaginary frequencies in the *cis* (501*i* cm^{-1}) and *trans* (456*i* cm^{-1}) species shows that the main vector lies along the N-O bond. The whole reaction leading to the formation of the final weakly bound adducts (**Dioxo_P**) between dioxomolybdenum complexes and trimethylamine is exothermic by 35.9 and 39.5 kcal mol^{-1} for the *cis* and *trans* isomers, respectively. Release of trimethylamine from the adducts (**Dioxo+P**) is accompanied by an energy gain of 3.1 kcal mol^{-1} along **Path a** and 2.9 kcal mol^{-1} along **Path b**.

The proposed mechanism[13] for the *trans*-attack involves that Me_3NO first approaches the Mo centre at the position *trans* to the oxo ligand to give an intermediate adduct. Then, the ligand moves to the *cis* position through a *trans*-*cis* rearrangement and the O-N bond is broken to afford a dioxomolybdenum(VI) complex. In spite of such indications, the effect of the *trans* attack explored in the present investigation does not reproduce (see Figure S4 of SI) what previously hypothesized.[13] Our calculations lead to a completely

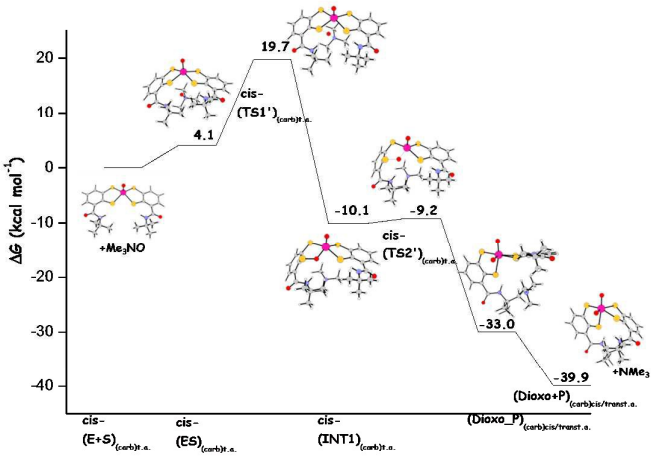

Figure 4. Calculated M06-L free energy profile for the **Me_3NO** *trans*-attack to the monooxomolybdenum(IV) **$E_{(carb)}$** complex in its *cis* arrangement. Energies are in kcal mol^{-1} and relative to reactants' asymptote.

different description of the reaction steps. That is, formation of a first adduct as a consequence of the *trans* to Mo=O approach of the substrate to the metal centre. The reaction proceeds by the transfer of the oxygen atom from the Me_3NO substrate to one sulphur atom and not, as suggested, to the Mo centre. The elongation of the S-O bond together with the shortening of the Mo-O bond and a reorganization of the ligands leads to the formation of the final dioxo products. The outcomes of our calculations confirm that, in accordance with what underscored above, molybdenum chemistry[37,38] does not permit the formation, though transient, of a linear dioxo species as a consequence of the *trans* attack. A final product where the dioxo moiety adopts a bent geometry around the metal centre is formed as the result of a series of steps that bypass the direct transfer of the oxygen atom to the Mo centre.

Concerning the identity of the dioxomolybdenum complex products formed along the examined pathways for both *cis*- and *trans*-attacks on *cis* and *trans* Mo(IV) complexes, the structures are reported in Figure 5.

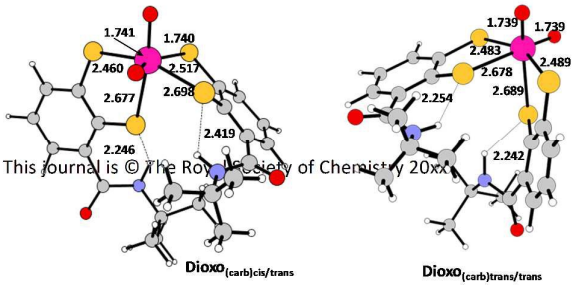

Figure 5. M06-L optimized structure of dioxomolybdenum(VI) complexes labelled as **$Dioxo_{(carb)cis/trans}$** and **$Dioxo_{(carb)trans/trans}$**. Most relevant geometrical parameters are reported. Bond lenghts are in Å and angles in degrees.

The *cis*-**$E_{(carb)}$** isomer leads to the formation of a complex, labelled **$Dioxo_{(carb)cis/trans}$**, in which one of the hydrogen-bonded thiolato ligand is *trans* to one of the Mo=O bonds and one is *cis* to the other oxo ligand. In the dioxo complex, indicated as **$Dioxo_{(carb)trans/trans}$**, formed along the calculated pathways describing the reactions of the *trans*-**$E_{(carb)}$** isomer, instead, both hydrogen-bonded thiolato ligands are *trans* to each of the oxo ligands. It is important to underline, for the sake of completeness, that when the attack to the *trans* isomer and consequent geometrical distortion occur from the side of the sulphur atom non involved in the hydrogen bond with the NH unit the **$Dioxo_{(carb)cis/cis}$** species is formed, that is less stable by about 4 kcal mol^{-1} than the most stable **$Dioxo_{(carb)trans/trans}$** one.

Okamura and co-workers[14], on the basis of the ^{1}H NMR results, and Raman analysis and DFT calculations concluded that the most stable dioxo isomer, in which both Mo=O bonds are *trans* to the hydrogen-bonded thiolato ligands, is the sole product. Furthermore, the strong donation of the oxo ligand at the *trans* position via *trans* influence should cause the elongation of the Mo-S bond and, conversely, the NH···S hydrogen bond should stabilize the longer Mo-S bond and strengthen the Mo=O bond at *trans* position. Such conclusions are only partially supported by the outcomes of our computational analysis. Indeed, the **$Dioxo_{(carb)trans/trans}$** isomer is calculated to be more stable than the **$Dioxo_{(carb)cis/trans}$** one by 2.5 kcal mol^{-1}. The Mo-S bond in *trans* to the M=O bond is elongated and, concurrently, the NH···S hydrogen bond is calculated to be stronger and shorter. However, in comparison with the structure of the dioxo product of the unsubstituted complex **E** the length of the Mo-O bond is not significantly influenced by the nature of the ligand in *trans*. Moreover, the **$Dioxo_{(carb)trans/trans}$** complex is not the sole product. All the efforts, carried out in order to rationalize the experimental evidence, to intercept a low energy transition state for the interconversion of the **$Dioxo_{(carb)cis/trans}$** isomer into the **$Dioxo_{(carb)trans/trans}$** one were unsuccessful. We were able to locate a transition state, whose structure is shown in Figure S6 of SI for the interconversion between the two *cis* and *trans* isomers of the initial monooxo **$E_{(carb)}$** complex. The height of the calculated energy barrier for such rearrangement is 27.4 kcal mol^{-1} in condensed phase. As a consequence, even if a rearrangement able to cause the transformation of the **$Dioxo_{(carb)cis/trans}$** into the **$Dioxo_{(carb)trans/trans}$** exists it should be very high energy demanding and should require the heating of the solution. As consequence, for both *cis* and *trans* monooxomolybdenum(IV) complexes, the Me_3NO attack to Mo at the position *cis* to the oxo ligand is more favorable than the attack at the *trans* one. The slowest step of this process is, such as for the unsubstituted complex, the formation of the first adduct. However, a comparison of the barrier calculated for the **E** complex (18.1 kcal mol^{-1}) and those for the *cis*-**$E_{(carb)}$** and *trans*-**$E_{(carb)}$** isomers calculated to be 14.4 and 15.3 kcal mol^{-1}, respectively confirms that the introduction of benzene substituents able to form intramolecular NH···S hydrogen bonds accelerates the Me_3NO reduction process.

3.2. Me_3NO reduction by the $[Mo(IV)O\text{-}(1,2\text{-}S2\text{-}3\text{-}t\text{-}BuCONHC_6H_3)_2]^{2-}$, $E_{(acylam)}$, complex

More recently, Okamura and co-workers[15] introduced at the 3-position of the 1,2-benzenedithiolato ligands a new series of acylamino groups (RCONH) designed and synthesized with the aim to provide a rigid and stable intraligand NH···S hydrogen bond and form a five-membered hydrogen bond that better reproduces the intraligand interaction in the natural enzyme molybdopterin cofactor (see Scheme 1). Also in this case the reaction pathways for both *cis* and *trans* isomers, indicated as *cis*-$\mathbf{E}_{(acylam)}$, and *trans*-$\mathbf{E}_{(acylam)}$, respectively were explored and for each isomer both *cis*- and *trans*-attack mechanisms were examined. M06-L free energy profiles illustrating the *cis*-attack leading to Me_3NO reduction by *cis*-$\mathbf{E}_{(acylam)}$ (**Path A**) and *trans*-$\mathbf{E}_{(acylam)}$ (**Path B**) complexes are depicted in Figure 6. Cartesian coordinates and the most relevant geometrical parameters of stationary points can be found in Table S4 and Figure S7, respectively of SI. Also for *cis*-$\mathbf{E}_{(acylam)}$, and *trans*-$\mathbf{E}_{(acylam)}$ species, *trans*-attack reaction steps are reported in the SI (Figure S8), where more detailed geometrical information and atomic Cartesian coordinates can be found (Figure S9 and Table S5, respectively).

At a first glance it clearly appears that the mechanistic steps for the Me_3NO *cis*-attack to both *cis*-$\mathbf{E}_{(acylam)}$ and *trans*-$\mathbf{E}_{(acylam)}$ complexes are very similar to those for the corresponding *cis* and

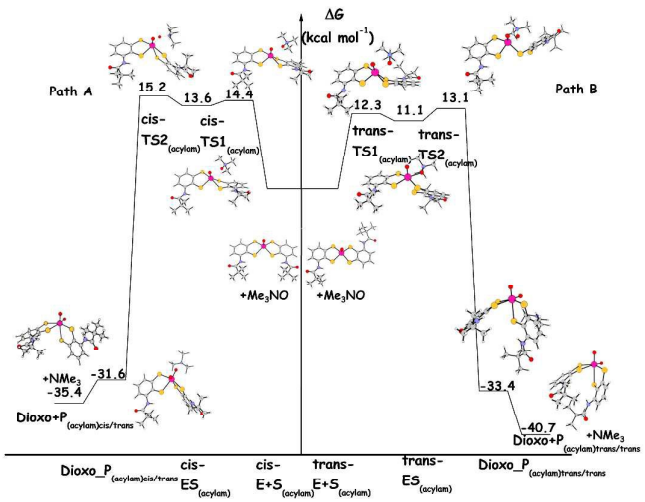

Figure 6. Calculated M06-L free energy profiles for the **Me_3NO** *cis*-attack to the monooxomolybdenum(IV) $\mathbf{E}_{(acylam)}$ complex in its *cis* (**Path A**) and *trans* (**Path B**) arrangements. Energies are in kcal mol^{-1} and relative to reactants' asymptote.

trans carbamoyl complexes and also the energetics do not differ significantly. In analogy with the results reported above, the attack to the *cis* isomer takes place from the less hindered side and, preferably, from the side of the hydrogen-bonded sulphur in the case of the *trans* isomer. The fully optimized structures of the two *cis*-$\mathbf{E}_{(acylam)}$ and *trans*-$\mathbf{E}_{(acylam)}$ minima are calculated to be isoenergetic. The substrate enters the Mo coordination sphere overcoming an energy barrier of 14.4 and 12.3 kcal mol^{-1} along the **Path A** for the *cis* isomer and **Path B** for the *trans* one, respectively. The formed adducts are slightly more stable, by 1.2 and 0.8 kcal mol^{-1} along **Path A** and **Path B**, respectively than the previous transition states. The formed adducts lead to the formation of the corresponding dioxomolybdenum(VI) products by the definitive oxygen atom transfer through two transition states with energy barriers of 1.6 kcal mol^{-1} along **Path A** and 2.0 kcal mol^{-1} along **Path B**. Dioxomolybdenum(VI) complexes formation is exothermic by 31.6 kcal mol^{-1} for the *cis* isomer and 33.4 kcal mol^{-1} for the *trans* one. Finally, the two dioxo complexes release the trimethylammine product with an energy gain of about 3.8 kcal mol^{-1} in the former case and 7.3 kcal mol^{-1} in the latter.

The examination of the mechanism of the Me_3NO attack to Mo at the *trans* to the oxo ligand position, gives results superimposable to those previously described for the *cis*-$\mathbf{E}_{(carb)}$ and *trans*-$\mathbf{E}_{(carb)}$ carbamoyl complexes. An initial oxygen atom transfer to a sulphur atom is involved that avoids the direct transfer to the Mo centre.

In analogy to what happens in the case of complexes with carbamoyl substituents, along both *cis*- and *trans*-attack pathways two dioxo isomers are obtained. The difference in energy between them is 5.3 kcal mol^{-1} and is due to the different disposition of the t-BuCONH groups on thiolate ligands. Indeed, the complex formed along the pathways for the Me_3NO attack to the *cis*-$\mathbf{E}_{(acylam)}$ complex is the isomer in which one of the hydrogen-bonded thiolato ligand is *trans* to one of the Mo=O bonds and the other is *cis* to the second oxo ligand. In analogy with the labeling adopted in the previous section, such isomer will be indicated as **Dioxo**$_{(acylam)cis/trans}$. Both Mo=O bonds are *trans* to the hydrogen-bonded thiolato ligands, instead, in the complex, labeled **Dioxo**$_{(acylam)trans/trans}$, formed by oxidation of the *trans*-$\mathbf{E}_{(acylam)}$ complex. Fully optimized structures and most relevant geometrical parameters for these two complexes are shown in Figure 7.

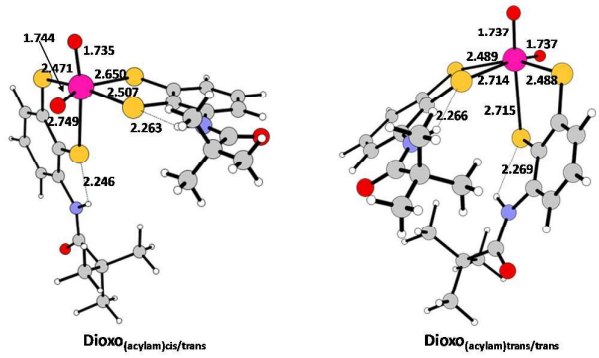

Figure 7. M06-L optimized structure of dioxomolybdenum(VI) complexes labelled as **Dioxo**$_{(acylam)cis/trans}$ and **Dioxo**$_{(acylam)trans/trans}$. Most relevant geometrical parameters are reported. Bond lengths are in Å and angles in degrees.

Results confirm that, in comparison with the Mo-O and Mo-S bond lengths calculated for the unsubstituted **E** and carbamoyl $\mathbf{E}_{(carb)}$ complexes, NH···S hydrogen bonds in *trans* position strengthen the Mo-O and weaken the S-O bonds. The *cis*-attack is more favorable than the *trans* one. The introduction of benzene substituents able to form intramolecular NH···S hydrogen bonds influences the course of the reaction as it appears from the calculated values of the energy barriers for the rate determining step, 14.4 and 12.3 kcal mol^{-1} for the *cis* and *trans* isomers, respectively with respect to 18.1 kcal mol^{-1} for the **E** complex.

Once again, we underscore that when the attack to the *trans* isomer from the side of the sulphur atom non involved in the hydrogen bond with the NH unit is explored, the dioxo product **Dioxo$_{(acylam)cis/cis}$** is formed that is less stable by about 4 kcal mol^{-1} than the most stable **Dioxo$_{(acylam)trans/trans}$** one.

4. Discussion

The results of our computational analysis illustrated in the previous section show that for all the examined monooxomolybdenum(IV) benzenedithiolato complexes the oxo transfer reaction from Me_3NO to form the corresponding dioxomolybdenum(VI) products occurs by the attack to the Mo centre at the position *cis* to the oxo ligand. However, relevant differences in behaviour exist due to the introduction of benzene substituents able to form NH···S hydrogen bonds. NBO charge analysis[34,35] is helpful in rationalizing this behavior. In Table 1 are collected the charges on each of the sulphur atoms for the investigated complexes. The oxygen atom of Me_3NO substrate carries a negative charge (-0.727 |e|), as well as negative is the charge on the Mo centre as a consequence of ligands donation. When Me_3NO approaches the complex in *cis* position to the oxo ligand is the sulphur atom in *trans* position to it that allows to delocalize the negative charge. In addition, the weakening and elongation of the bond between the Mo centre and the next hydrogen bonded S atom facilitates the distortion of the ligand.

Table 1. NBO analysis of charge density distribution for the investigated complexes.

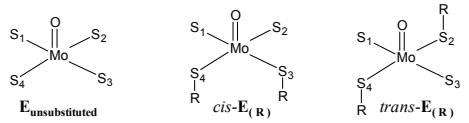

E$_{unsubstituted}$ *cis*-**E$_{(R)}$** *trans*-**E$_{(R)}$**

NBO					
	E$_{unsubstituted}$	Cis-E$_{(carb)}$	Trans-E$_{(carb)}$	Cis-E$_{(acylam)}$	Trans-E$_{(acylam)}$
Mo	-0.145	-0.149	-0.146	-0.172	-0.171
S_1	-0.016	0.015	0.004	-0.031	-0.037
S_2	-0.016	0.014	-0.007	-0.031	-0.061
S_3	-0.016	-0.016	0.004	-0.067	-0.037
S_4	-0.016	-0.020	-0.014	-0.067	-0.061

This is the reason why the barrier of the rate-determining step of the *cis*-attack mechanism lowers in going from **E** ($\Delta E^{\#}$=18.1 kcal mol^{-1}) to *trans*-**E$_{(carb)}$** ($\Delta E^{\#}$=15.3 kcal mol^{-1}) and *trans*-**E$_{(acylam)}$** ($\Delta E^{\#}$=12.3 kcal mol^{-1}). The rate-determining step barrier of the *cis*-attack mechanism, instead, becomes 14.4 kcal mol^{-1} for both *cis*-**E$_{(carb)}$** and *cis*-**E$_{(acylam)}$** as the attack occurs from the side of the sulphur atoms non involved in the hydrogen bond due to the steric hindrance of the benzene substituents in conjunction with the positive charge on such sulphur atoms. It is noteworthy that such results confirm the experimental suggestion that t-BuCONH acylamino groups are more effective in enhancing the reactivity owing to the greater rigidity and stability of the formed intraligand NH···S hydrogen bonds. A further support to this assumption comes from the calculated energy differences in exothermicity, reported above, of the formation of dioxo products, **Dioxo$_{(carb)}$** and **Dioxo$_{(acylam)}$**, in their *cis*/*trans* and *trans*/*trans* arrangements. Indeed, the **Dioxo$_{(carb)trans/trans}$** isomer is calculated to be more stable than the **Dioxo$_{(carb)cis/trans}$** by 2.5 kcal mol^{-1}, whereas the **Dioxo$_{(acylam)trans/trans}$** isomer is stabilized by 5.3 kcal mol^{-1}with respect the **Dioxo$_{(acylam)cis/trans}$**.

Another important difference is that for both substituted **E$_{(carb)}$** and **E$_{(acylam)}$** complexes the *trans*-attack, even if less viable with respect to the *cis*-attack, can occur whereas for the **E** complex such attack is precluded. As already underlined above, the *trans*-attack cannot lead to the formation of a linear O-Mo-O arrangement. Therefore, for both substituted **E$_{(carb)}$** and **E$_{(acylam)}$** complexes the attack is redirected towards the sulphur atoms. The explanation of this difference in behaviour can be ascribed to the ability of sulphur atoms in substituted thiolates to delocalize the excess of negative charge.

5. Conclusions

In this paper, we performed a theoretical comparative analysis of the mechanistic aspects of the reduction reaction of trimethylamine N-oxide by bioinspired catalysts namely monooxomolybdenum(IV) benzenedithiolato complex and its derivatives carrying on benzene rings carbamoyl (t-BuNHCO) and acylamino (t-BuCONH) substituents in both *cis* and *trans* arrangements. The two most accredited mechanisms of attack were explored, that is attack of the Me_3NO substrate at *cis* and *trans* positions, respectively with respect the oxo ligand.

The theoretical exploration of the reaction pathways revealed that the *cis*-attack is the preferred mechanism for all the compounds under investigation, whereas the way of attack at the *trans* position is energetically unfavourable and in the case of unsubstituted monooxomolybdoenzyme does not take place.

The reaction along the pathway for the *cis*-attack evolves through the approach of the substrate to the Mo centre in *cis* to the oxo ligand. Therefore, a distortion of the initial square-pyramidal geometry of the complex is observed. As a consequence, an energy barrier has to be overcome corresponding to the movement of one of the sulphur atoms from its position to allow the oxygen atom of Me_3NO to enter the coordination sphere of the Mo centre. This step represents the rate-determining step for all the investigated compounds. The reaction proceeds by definitive breaking of the N-O bond and formation of a new Mo-O bond in the formed adduct. Very low barriers are required for this step leading to the exothermic formation of an adduct between the dioxo(VI) complex and trimethylammine. Final release of trimethylammine and formation of separated products causes further stabilization.

Concerning the details of the *trans*-attack, from our calculations emerges that the oxygen atom is transferred before to a sulphur atom and in the next step to the metal centre with a concomitant reorganization in the coordination sphere of the ligands. This result confirms that, according to the molybdenum chemistry, formation of a linear dioxo species is not allowed and the assistance of a sulphur atom is required.

The investigation of the influence on the course of the reaction of the presence of substituents on the benzene ring able to form intramolecular NH···S hydrogen bonds confirms, according to experimental findings, that such interactions contribute to the reactivity tuning of the molybdoenzyme models and cause an acceleration of the substrate reduction.

Acknowledgements

This research was supported by Università della Calabria and FP7- PEOPLE-2011-IRSES, Project no. 295172. Mariagrazia Fortino gratefully acknowledges Commissione Europea, Fondo Sociale Europeo, Regione Calabria for the financial support.

Notes and references

1 V. L. Schramm *Chem. Rev.* 2006**, 106**, 3029-3030.
2 R. Wolfenden and M. J. Snider, *Acc. Chem. Res.* 2001, **34**, 938–945
3 M. R. A. Blomberg, T. Borowski, F. Himo, R.-Z. Liao and P. E. M. Siegbahn, *Chem. Rev.* 2014, **114**, 3601–3658.
4 S. F. Sousa, P. A. Fernandes and M. J. Ramos, *Phys. Chem. Chem. Phys.* 2012, **14,** 12431-12441.
5 S. P. de Visser, M. G. Quesne, B. Martin, P. Comba, U. Ryde, *Chem. Commun.*, 2014, **50**, 262-282.
6 F. Yu, V. M. Cangelosi, M. L. Zastrow, M. Tegoni, J. S. Plegaria, A. G. Tebo, C. S. Mocny, L. Ruckthong, H. Qayyum and V. L. Pecoraro, *Chem. Rev.* 2014, **114**, 3495–3578.
7 V. M. Robles, E. Ortega-Carrasco, L. Alonso-Cotchico, J. Rodriguez-Guerra, A. Lledós and J.-D. Maréchal, *ACS Catal*. 2015, **5**, 2469–2480.
8 D. N. Bolon and S. L. Mayo, *Proc. Natl. Acad. Sci. U.S.A.* 2001, **98**, 14274- 14279.
9 C. M. Thomas and T. R. Ward, *Chem. Soc. Rev.* 2005,**34**, 337–346
10 S. Chakraborty, P. Hosseinzadeh, Y. Lu, Encyclopedia of Inorganic and Bioinorganic Chemistry (Ed.: R.A. Scott) John Wiley and Sons, Ltd., Chichester, 2014, pp. 1-51.
11 S. W. Ragsdale *Chem. Rev.* 2006, **106**, 3317−3337
12 H. Oku, N. Ueyama, M. Kondo and A. Nakamura, *Inorg. Chem.* 1994, **33**, 209−216.
13 K. Baba, T. Okamura, C. Suzuki, H. Yamamoto, T. Yamamoto, M. Ohama and N. Ueyama, *Inorg. Chem.* 2006, **45**, 894−901.
14 T. Okamura, M. Tatsumi, Y. Omi, H. Yamamoto and K. Onitsuka, *Inorg. Chem.* 2012, **51**, 11688−11697.
15 T. Okamura, Y. Ushijima, Y. Omi and K. Onitsuka, *Inorg. Chem.* 2013, **52**, 381−394.
16 M Czjzek, Jean-Philippe Dos Santos, J. Pommier, G. Giordano, V. Méjean and R. Haser, *J. Mol. Biol.* 1998, **284**, 435-447.
17 R. Hille, J. Hall and P. Basu *Chem. Rev.* 2014, **114**, 3963-4038.
18 C. Lorber, M. R. Plutino, L. I. Elding and E. Nordlander, *J. Chem. Soc. Dalton Trans.*, 1997, 3997–4003.
19 N. M. F. S. A. Cerqueira, B. Pakhira and S. Sarkar, *J. Biol. Inorg. Chem.* 2015, **20**, 323-335.
20 A. L. Tenderholt, K. O. Hodgson, B. Hedman, R. H. Holm and E. I. Solomon *Inorg. Chem.* 2012, **51**, 3436-3442.
21 G. Moula, M. Bose and S. Sarkar *Inorg. Chem.* 2013, **52**, 5316−5327.
22 M. Leopoldini, N. Russo, M. Toscano, M. Dulak, T. A. Wesolowski, *Chem. Eur. J.* 2006, **12**, 2532-2541.
23 M. Leopoldini, S. G. Chiodo, M. Toscano and N. Russo, *Chem. Eur. J.* 2008, **14**, 8674-8681.
24 Gaussian 09, Revision D.01, M. J. Frisch, G. W. Trucks, H. B. Schlegel, G. E. Scuseria, M. A. Robb, J. R. Cheeseman, G. Scalmani, V. Barone, B. Mennucci, G. A. Petersson, H. Nakatsuji, M. Caricato, X. Li, H. P. Hratchian, A. F. Izmaylov, J. Bloino, G. Zheng, J. L. Sonnenberg, M. Hada, M. Ehara, K. Toyota, R. Fukuda, J. Hasegawa, M. Ishida, T. Nakajima, Y. Honda, O. Kitao, H. Nakai, T. Vreven, J. A. Montgomery, Jr., J. E. Peralta, F. Ogliaro, M. Bearpark, J. J. Heyd, E. Brothers, K. N. Kudin, V. N. Staroverov, R. Kobayashi, J. Normand, K. Raghavachari, A. Rendell, J. C. Burant, S. S. Iyengar, J. Tomasi, M. Cossi, N. Rega, J. M. Millam, M. Klene, J. E. Knox, J. B. Cross, V. Bakken, C. Adamo, J. Jaramillo, R. Gomperts, R. E. Stratmann, O. Yazyev, A. J. Austin, R. Cammi, C. Pomelli, J. W. Ochterski, R. L. Martin, K. Morokuma, V. G. Zakrzewski, G. A. Voth, P. Salvador, J. J. Dannenberg, S. Dapprich, A. D. Daniels, Ö. Farkas, J. B. Foresman, J. V. Ortiz, J. Cioslowski, and D. J. Fox, Gaussian, Inc., Wallingford CT, 2009.
25 Y. Zhao and D. G. Truhlar, *J. Chem. Phys.* 2006, **125**, 194101.
26 Y. Zhao and D. G. Truhlar, *Acc. Chem. Res.* 2008, **41**, 157-167.
27 A.D. Becke *Phys. Rev. B*, 1988, **38**, 3098.
28 C. Lee, W. Yang and R.G. Parr *Phys. Rev. B*, 1988, **37**, 785.
29 M. Swart, A.W. Ehlers and K. Lammertsma, *Molec. Phys.* 2004, **102**, 2467.
30 D. Andrae, U. Haussermann, M. Dolg, H. Stoll and H. Preuss, *Theor. Chim. Acta* 1990, **77**, 123-141.
31 K. Fukui, *J. Phys. Chem.* 1970, **74**, 4161-4163.
32 C. Gonzalez and H. B. Schlegel, *J. Chem. Phys.* 1989, **90**, 2154-2161.
33 A. V. Mareich, C. A. V. Marenich, C. J. Cramer and D. G. Truhlar, *J. Phys. Chem. B*, 2009, **113**, 6378-6396.
34 E. D. Glendening, J. E. Reed, J. E. Carpenter and F. Weinhold, NBO Program 3.1; Madison, WI, 1988.
35 A. E. Reed, L. A. Curtiss and F. Weinhold, *Chem. Rev.* 1988, ***88***, 899-926.
36 H. Sugimoto, S. Tatemoto, K. Suyama, H. Miyake, S. Itoh, C. Dong, J. Yang and M. L. Kirk, *Inorg. Chem.* 2009, **48**, 10581-10590.
37 R. H. Holm *Chem. Rev.* 1987, **87**, 1401-1449.
38 K. Tatsumi, and R. Hoffmann *Inorg. Chem.,* **19**, 1980, 2656-2658.

Graphical Abstract